Volume 1 | Number 1 | Jan 2013 | Pages 1–100

Analyst

www.rsc.org/analyst

ROYAL SOCIETY OF CHEMISTRY

ROYAL SOCIETY OF CHEMISTRY

www.rsc.org/analyst

Stereospecific recognition and quantitative structure-activity relationship between antibodies and enantiomers: ofloxacin as model hapten

Hong-tao Mu [a, §], Bao-ling Wang [a], Zhenlin Xu [a], Yuan-ming Sun [a], Xin-an Huang [b], Yu-dong Shen [a], Sergei A. Eremin [c,d], Anatoly V. Zherdev [c], Hong-tao Lei [a,*], Boris B. Dzantiev [c,*]

[a] Guangdong Provincial Key Laboratory of Food Quality and Safety, South China Agricultural University / Guangdong Provincial Engineering & Technique Research Centre of Food Safety Detection and Risk Assessment, Guangzhou 510642, China

[b] Tropical Medicine Institute, Guangzhou University of Chinese Medicine, Guangzhou 510405, China

[c] A.N. Bach Institute of Biochemistry, Russian Academy of Sciences, Moscow 119071, Russia

[d] Faculty of Chemistry, M.V. Lomonosov Moscow State University, 119991 Moscow, Russia

[*] **Corresponding authors** Tel: +86 20 8528 3448, Fax: +86 20 8528 0270, E-mail: immunoassay@126.com (Hongtao Lei); Tel: +7 495 954 3142, Fax: +7 495 954 2804, E-mail: dzantiev@inbi.ras.ru (Boris B. Dzantiev)

[§] Present address: College of Biology and Food Engineering, Guangdong University of Education, Guangzhou 510303, China

Abstract:

In this study, ofloxacin stereoisomers were chosen as a simple model to investigate the sterospecific recognition of chiral haptens and antibodies. Three polyclonal antibodies were raised and showed a relatively high enantioselectivity and an excellent sensitivity. Comparative molecular field analysis, and comparative molecular similarity indices analysis were employed to investigate the chiral recognition between antibody and ofloxacin enantiomer, and all the models yield high correlation and predictive ability. It was found that chiral discrimination probably caused by steric hindrance; the antibody sterospecificity could be ascribed to the variation of R_1 and R_3 groups of quinolones; the common structure of quinolones is also essential in the hapten-antibody recognition. The recognition between chiral haptens and antibodies were co-affected by multiple interaction forces, and those forces were defined explicitly at sub-structure level. An illustrative enhanced model with good simplicity and universality was also developed for better understanding the sterospecific recognition of ofloxacin enantiomers and antibodies for the first time. This work provides insights into the sterospecific recognition of chiral hapten and antibody.

Introduction

Enantioselective immunoassay is becoming one of the most important fields in analytical chemistry especially for clinical analysis, pharmaceutical analysis, food analysis, and environmental monitoring, due to the enantiomer can be determined without prior separation, directly from the matrix, with only dissolution and dilution.[1] To establish enantioselective immunoassays, high stereoselective antibodies must be available. Enantiomers often small molecules should be conjugated with carrier proteins to obtain immunogenicity during antibody preparation.[2] Thus, immunogen design is considered as the key step in anti-hapten antibody development.[3] However, hapten design especially chiral hapten design is still primarily based on the immunochemists' experiences and "trial and error" approach. This limitation should be blamed on the lack of understanding of chiral interactions between hapten and antibody.[2]

The key step in chiral recognition is the formation of diastereoisomeric complexes between the enantiomers and an antibody. The differences in Gibbs free energy between the two diastereoisomeric enantiomer-antibody complexes makes the chiral recognition results.[4] In 1933, Easson and Stedman were working on quantitative structure-activity relationships (QSAR) when they proposed that a minimum of three points of attachment were needed between a dissymmetric drug and its target to explain the different physiological activities ("three-point attachment model" which has been intensively used for chiral recognition explanation).[5] According to this

model, when three groups (a, b, c) of the tetrahedral carbon atom bind to a receptor surface at specific sites A, B, and C it is impossible that the enantiomer undergoes an equivalent binding via the same three-contact points.[6] The major drawbacks of this model are the two-dimensionality of the protein binding site, and the notion that all interactions between receptor and ligand are attractive.[7] Nowadays it is common agreement that not all three interactions need to be attractive, but both attractive and repulsive interactions are equivalent forces in generating stereoselectivity. For example, two of the interactions can be repulsive if the third one is strong enough to promote the formation of at least one of the two diastereomeric complexes.[8]

Later on, based on "six-center interactions" model,[9] Topiol and Sabio proposed an eight-center (four-contact point) interaction model,[10] which claimed that chiral recognition requires at least eight centers. The eight-center forces at the four-contact points could be either attractive or repulsive. But this model seems to be less illustrative.

Mesecar and Koshland introduced a four-location model to explain the binding of two of the four possible stereoisomers of isocitrate to the enzyme isocitrate dehydrogenase.[11] This four-location model declared that it is not necessary for there to be four binding sites. The four locations can, for example, be four attachment sites or three attachment sites and a direction, but a minimum of four designated locations are needed.[11] The four-location model was illustrated as Figure 1. Although the chiral recognition mechanism has been studied for several decades, the stereoselective model still in the progress of evolving.

4

A number of techniques have been utilized to explore the interaction of a variety of chiral ligands with their respective protein binding partners. Among these, X-ray crystallography has been commonly used to study stereoselectivity of proteins. In recent years, molecular modeling method especially QSAR approaches were adopted by immunochemists for some preliminary guidance on immunoassay development.[12, 13] The most widely used QSAR methods are traditional two-dimensional QSAR (2D-QSAR) based on the Hansch method and three-dimensional QSAR (3D-QSAR), such as comparative molecular field analysis (CoMFA) and comparative molecular similarity indices analysis (CoMSIA).[13] Those approaches showed great power in cross-reactivity (CR) prediction[14, 15], explanation[3, 16, 17], hapten design[18] and hapten-antibody recognition[2, 3, 19]. Although there were several QSAR studies carried out on antigen-antibody interaction studies,[13] recognition between chiral hapten and sterospecific antibody has not been seldom reported. In previous studies, whole molecular structures were employed in modelling in most cases,[13] while the effects of substructures rarely received much attention especially in chiral hapten-antibody recognition.

Ofloxacin is a broad-spectrum antibiotic of the quinolones (QNs) drug class commonly used in human and veterinary medicine to prevent or to treat bacterial infections throughout the world.[20] Ofloxacin is a chiral molecule and has two optical isomers differing in biological activity, i. e. *S*-(-)-ofloxacin (*S*-OFL) and *R*-(+)-ofloxacin (*R*-OFL) (Fig. 2). In our previous work, immunochromatographic assay for ofloxacin is proposed,[21] but the interaction between chiral hapten and

5

antibody was not involved. In this study, ofloxacin enantiomers were chosen as a model to study chiral recognition between hapten and antibody. Ofloxacin isomer is ideal model for chiral recognition study, not only because the chiral center lies in the border of rigid common structure of ofloxacin, but also the chiral center composed of two simple groups (methyl and hydrogen). In this investigation, three sterospecific rabbit polyclonal antibodies (pAbs) were raised against racemic-ofloxacin (*rac*-OFL), *S*-OFL, and *R*-OFL, respectively. The sensitivity, enantioselectivity, and specificity of three enantioselective pAbs were characterized using the indirect competitive enzyme-linked immunosorbent assay (icELISA). In order to obtain insights into the chiral recognition between ofloxacin isomers and antibodies in molecular level, CoMFA and CoMSIA approaches were carried out based on cross-reactivity data. This investigation further developed the famous four-location theory in chiral recognition mechanism, and this would give a more comprehensive understanding to hapten-antibody recognition.

Experimental

Chemicals and buffers

R-OFL (purity, ≥ 98%), *S*-OFL (≥ 98%), *R*-OFL methyl ester (*S*-OFLM) and *R*-OFL methyl ester (*R*-OFLM) standards were obtained from Daicel chiral technologies company (Shanghai, China). Rufloxacin (RUF), *rac*-OFL, garenoxacin (GAR), marbofloxacin (MAR), pefloxacin (PEF), norfloxacin (NOR), clinafloxacin (CLI), enrofloxacin (ENR), difloxacin (DIF), pipemidic acid (PIP), moxifloxacin (MOX), lomefloxacin (LOM), pazufloxacin (PAZ), gatifloxacin (GAT), sarafloxacin

(SAR), tosufloxacin (TOS), ciprofloxacin (CIP), sparfloxacin (SPA), nalidixic acid (NAL), prulifloxacin (PRU), oxolinic acid (OXO) were supplied by Veterinary Medicine Supervisory Institute of China (Beijing, China). The structures of related QNs were shown in Fig. 2. Bovine serum albumin (BSA), ovalbumin (OVA), N-hydroxysuccinimide (NHS), N,N'-dicyclohexylcarbodiimide (DCC), 3,3′,5,5′-tetramethylbenzidine (TMB), HRP conjugated goat anti-rabbit IgG (HRP-IgG), incomplete Freund's adjuvant (IFA), complete Freund's adjuvant (CFA) were purchased from Sigma-Aldrich (Missouri, USA). All other chemicals and solvents were analytical grade or better. Deionized water was prepared using a Milli-Q water purification system (Millipore, Bedford, MA). Female New Zealand white rabbits weighing 1.0-2.0 kg were obtained from Guangdong Medical Laboratory Animal Center (Guangzhou, China). 96 microtiter plates for ELISA were obtained from Yunpeng Technology Development Co., Ltd, (Xiamen, China).

Carbonate buffer (0.05 mol L^{-1}, pH 9.6) was used for coating plates. 0.01 mol L^{-1} PBST solution (0.01 mol L^{-1} phosphate buffer saline (PBS, pH 7.4) containing 0.1% Tween-20) was used for washing plate. 0.5% skim milk powder (diluted with PBS) was used to block each well. 0.04 mol L^{-1} phosphate-citrate buffer (pH 5.5) was used as substrate buffer. The substrate buffer contains 0.01% TMB and 0.004% H_2O_2 were used as solution for HRP colorimetric detection.

Instrumentation and supplies

Ultraviolet-visible (UV-Vis) spectra were recorded on a UV-160A Shimadzu spectrophotometer (Kyoto, Japan). ELISA plates were washed using a Multiskan

7

MK2 microplate washer (Thermo Labsystems, USA). Absorbance reading was carried out at wavelength of 450 nm using a Multiskan MK3 microplate reader (Thermo Fisher Scientific, Pittsburgh, USA). The IC_{50} was analyzed with Logistic equation using the OriginPro 8.0 software (OriginLab Corporation, Northampton, MA). The molecular modeling was conducted with SYBYL-X 2.0 software package (Tripos Inc., USA) running on a personal computer.

Hapten-protein conjugates preparation and pAbs production

Ofloxacin isomers and racemic mixture were coupled to carrier proteins (BSA and OVA) using NHS ester method. *S*-OFL and *rac*-OFL protein conjugates were synthesized in our previous work.[21] *R*-OFL protein conjugates were synthesized in the same way. Briefly, *R*-OFL (4mg, 12.5 μmol) was dissolved in a mixture of 1 mL solution of DCC (25 μmol mL^{-1}) and NHS (25 μmol mL^{-1}) in anhydrous DMF, and incubated overnight at room temperature. This activated hapten (0.4 mL) was then assed dropwise with shaking to a OVA (15 mg, 0.25 μmol) or BSA (17 mg, 0.25 μmol) in 2 mL of cold 50 mmol L^{-1} carbonate buffer (pH 9.6) with 50 μL DMF, and then incubated at 4 °C overnight. Before used as immunogen or coating antigen, the hapten-protein conjugates were dialyzed against PBS at 4 °C for 72 h. BSA conjugates (*S*-OFL-BSA, *R*-OFL-BSA, and *rac*-OFL-BSA) were used as immunogens, and OVA conjugates (*S*-OFL-OVA, *R*-OFL-OVA, and *rac*-OFL-OVA) were used as coating antigens.

New Zealand white rabbits immunized with *rac*-OFL and *S*-OFL conjugates gave the pAb/*S*-OFL and pAb/*rac*-OFL antisera, respectively.[21] Antiserum against *R*-OFL

was prepared in the same way, and was named pAb/*R*-OFL. All the blood samples were collected directly from the heart and clotted at 4 °C for 12 h, then centrifuged at 3000 rpm for 10 min. The pAbs were purified from antisera by ammonium sulfate precipitation and protein-G column. The concentrations of purified pAbs were determined with UV-vis spectrometry. The animals were fed and conducted according to principles of the Institutional Authority for Laboratory Animal Care.

Development of icELISA method

The icELISA method was established on the basis of the common protocol.[22] Hapten-OVA conjugate was coated to 96 microtiter plates (100 μL/well) at 4 °C for 12 h. After blocking with blocking buffer (120 μL/well) at 37 °C for 3h, the analytes and optimized dilutions of pAbs dissolved in PBST (100 μL/well for each) were added and then the plates were incubated at 37 °C for 40 min. After washes, 5000-fold IgG-HRP were added 100 μL/well and the plates were incubated at 37 °C for 30 min. TMB solution was added and incubated for 10 min at 37 °C. After each step, a PBST washing step was carried out. Color development was terminated with 50 μL 2 mol L^{-1} H$_2$SO$_4$ and the absorbance was recorded at a wavelength of 450 nm. The concentration of antibodies and coating antigens had been optimized using checkerboard titration and standard curves. The concentrations under which the assay got the highest valve of A$_{450max}$/ IC$_{50}$ were chosen as the working conditions.

Cross-reactivity

The specificity of the icELISA was determined using 24 QNs under optimized conditions. The CR values were calculated according to the following equation:

$$CR = (IC_{50(\text{hapten, mol L}^{-1})} / IC_{50(\text{cross-reactant, mol L}^{-1})}) \times 100 \qquad (1)$$

QSAR investigation

QSAR were all performed using the SYBYL-X 2.0 package. The 3D structures of 24 QNs were optimized to global low energy conformations using the standard Tripos force field in conjunction with Gasteiger-Hückel charges. The maximum interaction was 1000, and other parameters adopted default values. pIC_{50} defined as $-\log IC_{50}$ (in molar units), was used to indicate the activities of antibody recognition.

CoMFA and CoMSIA are famous in 3D-QSAR and they all need molecular alignment step. 24 structures of QNs were aligned based on the common structure 4-oxo-4,7-dihydroquinoline-3-carboxylic acids (Fig. 2). The biological data (pIC_{50}) activity values were used as dependent variable, and CoMFA or CoMSIA fields were used as independent variables. PLS with a leave-one-out (LOO) cross-validation was applied to build the model. The contour maps were finally generated according to the non-cross-validated model. In contour specifications, contour model was chosen by contribution, and display model was chosen as solid. All three pAbs activity data were performed in CoMFA and CoMSIA studies.

Results and discussion

PAb production and optimization of icELISA

Ofloxacin enantiomers are small organic molecules (MW = 361.37) that can elicit an immune response only when attached to a large carrier protein (BSA or OVA). Carboxylic acid group of ofloxacin and amino group of carrier protein can form a new

10

amido bond in presence of DCC and NHS. The obtained pAbs were characterized

using icELISA.

The optimized concentration of coating antigen and pAbs was determined

according to the standard homologous icELISA protocol. The optimized ELISA

procedure is described as below: 0.100 mg L^{-1} R-OFL-OVA and 0.050 mg L^{-1}

pAb/R-OFL obtained the best sensitivity (IC$_{50}$) with the maximum absorbance (A$_{max}$)

in the range of 0.9-1.2 (Table S1). In the same way, 0.013 mg L^{-1} S-OFL-OVA and

0.031 mg L^{-1} pAb/S-OFL were chosen as anti-S-OFL antibody's optimized conditions;

0.050 mg L^{-1} rac-OFL-OVA and 0.050 mg L^{-1} pAb/rac-OFL were selected as ideal

working conditions of anti-rac-OFL antibody (Table S1).

Enantioselectivity, sensitivity, and specificity of pAbs

Standard curves showed that pAb/R-OFL and pAb/S-OFL have enantioselectivity

while pAb/rac-OFL has no enantioselectivity (Fig. 3 and Table 1). pAb/R-OFL

selectively recognize R-OFL isomer (Fig. 3a). In competitive test of pAb/R-OFL, the

sensitivity (IC$_{50}$) to R-OFL (0.00119 μmol L^{-1}) was much lower than that of S-OFL

(0.01809 μmol L^{-1}), and the IC$_{50}$ to rac-OFL (0.00298 μmol L^{-1}) was intermediate.

CR values of R-, S-, and rac-OFL was 100.0%, 6.6%, 39.9%, respectively.

pAb/S-OFL selectively recognize S-OFL isomer (Fig. 3b). The inhibitory test of

pAb/S-OFL showed that the IC$_{50}$ to S-OFL (0.00083 μmol L^{-1}) was much lower than

that of R-OFL (0.00390 μmol L^{-1}), and the IC$_{50}$ to rac-OFL (0.00139 μmol L^{-1}) was

between that of other two. CR values of S-, R-, and rac-OFL was 100.0%, 21.3%,

59.9%, respectively. The overlapping calibration curves of pAb/rac-OFL against

11

ofloxacin and its enantiomers show that pAb/*rac*-OFL has almost the same selectivity to each optical isomer, and has no enantioselectivity (Fig. 3c). The IC_{50} of pAb/*rac*-OFL against *rac*-, *S*-, and *R*-OFL are 0.00058, 0.00048, and 0.00056 μmol L^{-1}, respectively. pAb/*rac*-OFL recognizes *R*-, *S*-, and *rac*-OFL as equal and have no discrimination ability to ofloxacin enantiomers. All the three pAbs have high sensitivity, especially for pAb/*S*-OFL and pAb/*rac*-OFL. The standard curves of three pAbs showed a low background (with an average A_{450} lower than 0.106), indicating no nonspecific binding was found in the test.

Although pAb/*S*-OFL and pAb/*R*-OFL have prominent chiral recognition, the enantioselectivities are limited. The reason may blame on the chiral center's composition and location. The chiral center is composed of two simple, small and uncharged groups: chiral methyl and hydrogen. The only difference between *R*-OFL and *S*-OFL is exchange of methyl and hydrogen. Those properties probably result in the low stereospecific affinity between *S* and *R* isomers. However, the simplicity of the chiral center make ofloxacin enantiomers ideal model for chiral recognition studies. At one hand the chiral center lies in the border of rigid common structure of ofloxacin, which make chiral methyl fully exposed during immune responses. At another hand, chiral methyl and hydrogen are the most ideal partners to reveal the important role of steric hindrance in chiral recognition.

Twenty four ofloxacin structural analogues were applied to evaluate the specificity of the pAbs, and the obtained IC_{50} values (μmol L^{-1}) were used to calculate CR value. The results show that all three pAbs have relatively high specificity (Table 1). In

12

general, except for ofloxacin and their derivatives (*R*-OFLM and *S*-OFLM), only RUF

and GAR had a high CR value (CR > 10%). Then the CR value of MAR and PEF

were between 1% and 10%, and other QNs' CRs were lower than 1% or even not

detected.

CoMFA

CoMFA and CoMSIA are most attractive 3D-QSAR methods to study the

recognition of chiral molecules especially when datasets of congeneric ligands were

studied.[23, 24] In CoMFA study, PLS analysis at their optimal number of principal

components (ONC = 2 for pAb/*R*-OFL, ONC = 3 for pAb/*S*-OFL, ONC = 4 for

pAb/*rac*-OFL) yielded high correlation (r^2 = 0.818 for pAb/*R*-OFL, r^2 = 0.905 for

pAb/*S*-OFL, r^2 = 0.959 for pAb/*rac*-OFL) and predictiveability (q^2 = 0.552 for

pAb/*R*-OFL, q^2 = 0.652 for pAb/*S*-OFL, q^2 = 0.670 for pAb/*rac*-OFL). Normally, the

cross-validation coefficient (q^2) is used as a criterion of both robustness and predictive

ability of the model. In many cases, a high q^2 value (usually > 0.5) is considered as an

indicator or even as the ultimate proof that the model is accurate or reliable.[25]

The std*coeff contour maps for the CoMFA models are shown in Fig. 4. Green and

yellow contours refer to sterically favored and unfavored regions. Blue and red

contours refer to regions where electron-donating and electron withdrawing groups

are favored. CoMFA contour plots showed that the hapten-antibody interactions of

three models are similar. It is easily seen from the fact that most contours were located

around the moiety of oxazine ring and the piperazinyl ring in the similar distribution

(Fig. 4). This also implied that the moiety of oxazine ring and the piperazinyl ring

played an important role in ofloxacin-antibody interaction. The distribution of yellow contours near to the chiral center shows that the steric hindrance affects enantioselectivity of pAbs directly. The green contour map near the methyl group of piperazinyl ring indicated this area where steric bulk is predicted to enhance the biological activity (Fig. 4 a1, b1, and c1). It can explain that GAR has a relatively high CR value in spite of large R_3 group. The blue maps beside the carboxy group of ofloxacin implied that the pAbs may recognize the linker of conjugates during immunization. There were blue plots near the common structure of QNs, which indicate that the common skeleton would interact with pAbs via electrostatic interactions.

It is generally recognized that hapten-carrier linking groups are less exposed to antibodies during immunization. Therefore, the moiety in the same position is widely considered to less contributive to a hapten-antibody interaction. However, as deduced in the force field (CoMFA) analysis, the methoxyl of *R*-, and *S*-OFLM was surrounded by blue contours, which suggest that the linker of the conjugates may also play an important role during immunization.

CoMSIA

CoMSIA models got good correlation ($r^2 = 0.995$ for pAb/*R*-OFL, $r^2 = 0.977$ for pAb/*S*-OFL, $r^2 = 0.988$ for pAb/*rac*-OFL) and predictiveability ($q^2 = 0.589$ for pAb/*R*-OFL, $q^2 = 0.627$ for pAb/*S*-OFL, $q^2 = 0.689$ for pAb/*rac*-OFL) at the optimal number of principal components (ONC = 10 for pAb/*R*-OFL, ONC = 5 for pAb/*S*-OFL, ONC = 5 for pAb/*rac*-OFL). The different field descriptors and the

14

optimal number of principal components (ONC) were optimized using LOO PLS, and the best q^2 models were used for r^2 calculation and contour map generation. The hydrophobic field contribution of model pAb/*R*-OFL, pAb/*S*-OFL, and pAb/*rac*-OFL were 52.6%, 31.2%, and 58.6%, respectively. It was indicated that the hydrophobic interaction was the critical point of the ofloxacin-antibody reaction. Other fields (steric, H-bond donor for pAb/*R*-OFL; steric, electrostatic, H-bond donor, H-bond acceptor for pAb/*S*-OFL; electrostatic, Hydrophobic for pAb/*rac*-OFL) also affected the antibody recognition. That is to say, different fields co-affected ofloxacin-antibody recognition.

The CoMSIA std*coeff contour maps shown in Fig. 5 supplied more information than that of CoMFA. Except for steric and electrostatic interactions, hydrophobic, H-bond donor and acceptor interactions were also taken into consideration. CoMSIA results were mainly agreed with that of CoMFA. The green and yellow maps around the chiral center showed that steric hindrance would be the reason of chiral recognition (Fig. 5 a1, b1 and c1). The green contour near the methyl of piperaxinyl group showed that large bulk in this area may favor the biological activity. The CoMSIA contour plots were also mainly close to the moiety of oxazine and the piperazinyl ring, which suggesting again that this moiety play an important part in ofloxacin-antibody recognition. The oxygen atom of oxazine ring plays an important role in recognition by forming hydrophilic and electrostatic attractions (Fig. 5 a2, b3, c3, b2, and c2). The piperazinyl ring interacts with pAbs by forming hydrophobic, hydrogen bond, and electrostatic attractions (Fig. 5 a2, b3, c3, a3, b4, b5, b2, and c2).

The common structure of QNs also contributes to ofloxacin-antibody recognition via hydrophobic and electrostatic interactions (Fig. 5 c3, b2, and c2).

Although most of the results getting from CoMFA and CoMSIA model are the same, there are some differences. For example, CoMFA results showed that the pAbs may recognize the conjugate linker, but the CoMSIA results didn't show this information. Whereas, CoMSIA models showed informations about hydrophobic, H-bond donor and H-bond acceptor, but CoMFA models didn't. In brief, using both CoMFA and CoMSIA methods for ofloxcin-antibody chiral recognition study can give us a more informative result, and those methods have complementary between each other in interaction study.

An enhanced model for antibody enantioselectivity

From the analysis of CoMFA and CoMSIA, the factors effected stereoselectivity of anti-ofloxacin antibody can be conclude that 1) the steric hindrance would be the reason which caused antibodies' chiral recognition, and the moiety of oxazine and the piperazinyl ring (R1 and R3 groups) play an important role in ofloxacin-antibody recognition; 2) parts of common skeleton of quinolone drugs would interact with pAbs during hapten-antibody recognition; 3) the linkage part of conjugates may also take part in molecular recognition during immunization; 4) The hydrophobic interaction is critical in ofloxacin-antibody reaction, and other force fields (such as steric force, hydrogen bonding interaction and electrostatic force) co-affected ofloxacin-antibody recognition. The interactions between ofloxacin isomers and antibodies can be illustrated as Fig. 6 (a, b). Briefly, the 4 groups (shown in oval dash

line) attached to the tetrahedral C12 atom of *R*-OFL interact with four locations (shown in gray oval) in the antibody's putative active site. Among those locations, groups b and c participate in chiral recognition mainly by steric hindrance, and groups a and d take part in chiral interaction mainly by interaction forces, such as electrostatic forces and hydrophobic forces (Fig. 4, 5). This result supported the four-location model proposed by Mesecar and Koshland[11] in 2000.

Although Mesecar and Koshland give an illustrated model, the model has some shortcomings in simplicity and universality. The reason may be lie in the model was illustrated exactly according to crystallographic data of complexed isocitrate dehydrogenase (combining with the cleft active site), and other combine patterns (binding to a flat protein surface from the top or binding to protruding residues) were not taking into consideration. Thus, we revised the illustrated model of four-location theory, and name it 'illustrative enhanced four-location model' (Fig. 6 c, d).

In the enhanced model, the active site of antibody was simplified as a putative corner. And chiral tetrahedral molecules located in the corner forming a minimum of four designated locations. The four locations can, for example, be four attachment sites or three attachment sites and a direction.[11] According to our study, the chiral tetrahedral molecule attaches to enantioselective antibody by interaction forces or steric hindrance, and merely a steric docking may form an attachment in chiral recognition, such as the chiral methyl of ofloxacin. If, for instance, there are three attaching sites and a fourth location, the vertical plate in the enhanced model merely represented the direction of this chiral tetrahedral molecule. In one location, various

17

interaction forces (hydrogen bonding interaction force, hydrophobic interaction force and electrostatic interaction force) may work together to form the attachment, such as piperazinyl moiety at R_3 position of ofloxacin. Another research by our group can be well explained by this illustrative enhanced model. The improved model give a better illustrating of four-location theory, and presents a deeper understanding of chiral recognition mechanism for both antibodies and other proteins.

Acknowledgements

References

1.   E. L. Izake, *J. Pharm. Sci.*, 2007, **96**, 1659-1676.

2.   M. Yuan, Y. Na, L. Li, B. Liu, W. Sheng, X. Lu, I. Kennedy, A. Crossan and

S. Wang, *J. Agric. Food Chem.*, 2012, **60**, 10486-10493.

3.   Z.-L. Xu, Y.-D. Shen, W.-X. Zheng, R. C. Beier, G.-M. Xie, J.-X. Dong, J.-Y. Yang, H. Wang, H.-T. Lei and Z.-G. She, *Anal. Chem.*, 2010, **82**, 9314-9321.

4.   A. Berthod, *Anal. Chem.*, 2006, **78**, 2093-2099.

5.   L. H. Easson and E. Stedman, *Biochem. J.*, 1933, **27**, 1257-1266.

6.   M. Lämmerhofer, *J. Chromatogr. A*, 2010, **1217**, 814-856.

7.   D. I. Ranieri, D. M. Corgliano, E. J. Franco, H. Hofstetter and O. Hofstetter, *Chirality*, 2008, **20**, 559-570.

8.   V. A. Davankov, *Chirality*, 1997, **9**, 99-102.

9.   L. Salem, X. Chapuisat, G. Segal, P. C. Hiberty, C. Minot, C. Leforestier and P. Sautet, *J. Am. Chem. Soc.*, 1987, **109**, 2887-2894.

10.   S. Topiol and M. Sabio, *J. Am. Chem. Soc.*, 1989, **111**, 4109-4110.

11.   A. D. Mesecar and D. E. Koshland, *Nature*, 2000, **403**, 614-615.

12.   M. F. Andrada, P. R. Duchowicz and E. A. Castro, *Curr. Org. Chem.*, 2013, **17**, 2872-2879.

13.   Z.-L. Xu, Y.-D. Shen, R. C. Beier, J.-Y. Yang, H.-T. Lei, H. Wang and Y.-M. Sun, *Anal. Chim. Acta*, 2009, **647**, 125-136.

14.   Y.-F. Zhang, Y. Ma, Z.-X. Gao and S.-G. Dai, *Anal. Bioanal. Chem.*, 2010, **397**, 2551-2557.

15.   Y. Li, Y. Liu, H. Chen, P. Wei and F. Li, *J.Mol. Biochem.*, 2012, **1**, 206-211.

16.   R. C. Beier and L. H. Stanker, *Anal. Chim. Acta*, 2001, **444**, 61-67.

17.   Z. Wang, Y. Zhu, S. Ding, F. He, R. C. Beier, J. Li, H. Jiang, C. Feng, Y. Wan

and S. Zhang, *Anal. Chem.*, 2007, **79**, 4471-4483.

18.   P. Sharma, M. Kukkar, A. K. Ganguli, A. Bhasin and C. R. Suri, *Analyst*, 2013, **138**, 4312-4320.

19.   M. Yuan, B. Liu, E. Liu, W. Sheng, Y. Zhang, A. Crossan, I. Kennedy and S. Wang, *Anal. Chem.*, 2011, **83**, 4767-4774.

20.   C. M. Oliphant and G. M. Green, *Am. Fam. Physician*, 2002, **65**, 455-464.

21.   N. A. Byzova, N. I. Smirnova, A. V. Zherdev, S. A. Eremin, I. A. Shanin, H.-T. Lei, Y. Sun and B. B. Dzantiev, *Talanta*, 2014, **119**, 125-132.

22.   Y. Gao, M. Yang, C. Peng, X. Li, R. Cai and Y. Qi, *Analyst*, 2012, **137**, 229-236.

23.   A. Plazinska, K. Pajak, E. Rutkowska, L. Jimenez, J. Kozocas, G. Koolpe, M. Tanga, L. Toll, I. W. Wainer and K. Jozwiak, *Bioorg. Med. Chem.*, 2014, **22**, 234-246.

24.   R. K. Verma, V. Kumar, P. Ghosh and L. K. Wadhwa, *Med. Chem. Res.*, 2013, **22**, 287-302.

25. A. Golbraikh and A. Tropsha, *J. Mol. Graphics Modell.*, 2002, **20**, 269-276.

Figure Legends

Fig. 1 Four-point location model for stereoselectivity of a protein, showing how a protein might provide two sites (D' and D'') in either of two locations for interaction with group D on a chiral carbon atom: D' would bind one enantiomer and D'' would bind its mirror image.[11]

Fig. 2 The structure of QNs involved in this study. The common structure of QNs is labeled in blue.

20

Fig. 3 Representative inhibition curves of pAb/*R*-OFL (a), pAb/*S*-OFL (b) and pAb/*rac*-OFL (c) by varying concentrations of free *S*-OFL(■), *rac*-OFL (●) and *R*-OFL(▲). Each point represents the mean ±SD (standard deviation) of three assays.

Fig. 4 CoMFA std*coeff contour plots of model pAb/*R*-OFL with *R*-OFL as reference molecule (a1, a2), pAb/*S*-OFL with *S*-OFL (b1, b2), and pAb/*rac*-OFL with *S*-OFL (c1, c2). In steric contour maps (a1, b1, and c1), green and yellow contours refer to sterically favored and unfavored regions; in electrostatic contour maps (a2, b2, and c2), blue and red contours refer to regions where electron-donating and electron withdrawing groups are favored.

Fig. 5 CoMSIA std*coeff contour plots of model pAb/*R*-OFL with *R*-OFL as reference molecule (a1-a3), pAb/*S*-OFL with *S*-OFL (b1-b5), and pAb/*rac*-OFL with *S*-OFL (c1-c3). In steric contour maps (a1, b1, and c1), green and yellow contours refer to sterically favored and unfavored regions; in electrostatic contour maps (b2, c2), blue and red contours refer to regions where electron-donating and electron withdrawing groups are favored; in hydrophobic contour maps (a2, b3, and c3), white and orange contours refer to regions where hydrophilic and hydrophobic substituents are favored; in hydrogen bond donor contour maps (a3, b4), the cyan and purple contours indicate favorable and unfavorable hydrogen bond donor groups; in hydrogen bond acceptor contour map (b5), the magenta and red contours demonstrated favorable and unfavorable hydrogen bond acceptor groups.

Fig. 6 Ofloxacin–antibody recognition model (a, b) and illustrative enhanced four-location model (c, d). The 4 groups attached to the tetrahedral C12 atom of

ofloxacin are labeled by oval dashed lines; meanwhile, corresponding binding sites on

antibody are represented by gray ovals. The dashed line in light blue represents

interactions between enantiomer and antibody.

Tables

Table 1 The IC_{50} values and cross-reactivities of the NQs against enantioselective antibodies. The values represented the mean of three separate experiments each of which contained a minimum of three replicates.
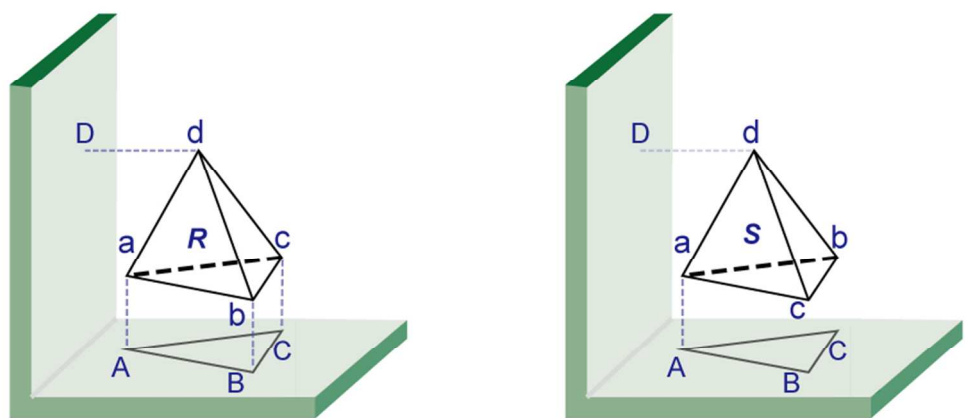
	pAb/*R*-OFL		pAb/*S*-OFL		pAb/*rac*-OFL	
	$IC_{50}{}^{a}$ (μmol L^{-1})	CR^{b}(%)	IC_{50}(μmol L^{-1})	CR (%)	IC_{50}(μmol L^{-1})	CR (%)
R-OFL	0.00119	100.0	0.00390	21.3	0.00056	104.1
rac-OFL	0.00298	39.9	0.00139	59.9	0.00058	100.0
S-OFL	0.01809	6. 6	0.00083	100.0	0.00048	121.4
R-OFLM	0.00088	135.5	0.00329	25.3	0.00058	99.7
S-OFLM	0.00508	23.4	0.00038	217.3	0.00061	94.9
RUF	0.00120	98.7	0.00176	47.2	0.00043	134.5
GAR	0.00186	63.9	0.00469	17.7	0.00144	40.5
MAR	0.02567	4.6	0.01039	8.0	0.00397	14.7
PEF	0.39538	0.3	0.06505	1.3	0.02719	2.1
NOR	0.79709	0.2	0.27924	0.3	0.13306	0.4
CLI	0.83021	0.1	0.41007	0.2	0.24617	0.2
ENR	0.89093	0.1	0.35028	0.2	0.07981	0.7
DIF	0.96423	0.1	0.30045	0.3	2.00259	< 0.1
PIP	1.04506	0.1	5.93433	< 0.1	7.91244	< 0.1
MOX	2.49103	< 0.1	2.52092	< 0.1	0.59487	0.1
LOM	2.70459	< 0.1	0.76846	0.1	0.39243	0.2
PAZ	6.28338	< 0.1	0.48517	0.2	0.35709	0.2
GAT	10.65530	< 0.1	1.46510	< 0.1	1.05858	< 0.1
SAR	12.97454	< 0.1	2.33542	< 0.1	0.79759	< 0.1
TOS	ND^{c}	ND	1.73117	< 0.1	0.49462	0.1
CIP	ND	ND	6.03591	< 0.1	1.50898	< 0.1
SPA	ND	ND	ND	ND	ND	ND
NAL	ND	ND	ND	ND	4.30589	< 0.1
PRU	ND	ND	ND	ND	4.55077	< 0.1
OXO	ND	ND	ND	ND	ND	ND

^{a} The values of IC_{50} (μmol L^{-1}) were obtained from four-parameter logistic equations used to fit standard curves and were the mean of triplicate experiments.

^{b} CR means cross-reactivity.

^{c} ND means Not Detected.

Graphical Abstract
76x34mm (300 x 300 DPI)

1
2
3
4
5
6
7
8
9
10
11
12
13
14
15
16
17
18
19
20
21
22
23
24
25
26
27
28
29
30
31
32
33
34
35
36
37
38
39
40
41
42
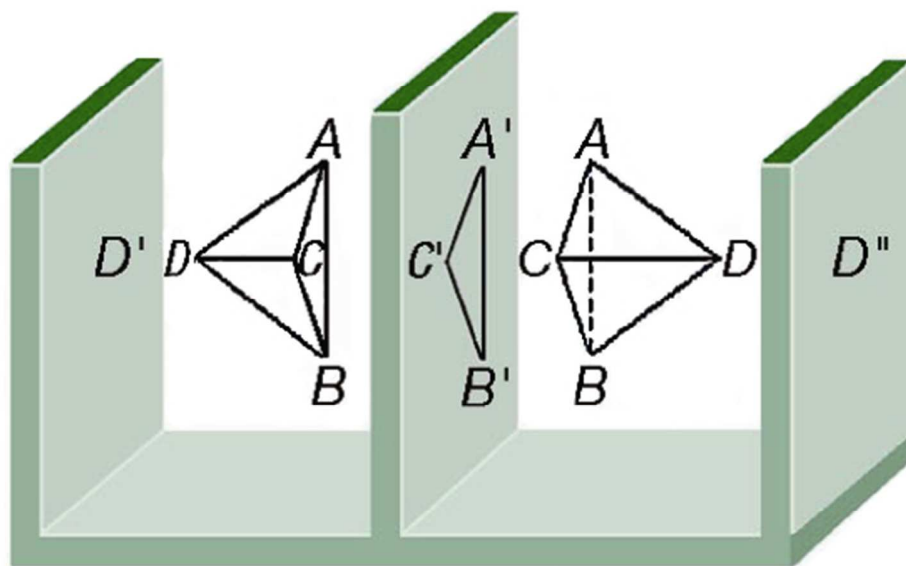43
44
45
46
47
48
49
50
51
52
53
54
55
56
57
58
59
60

Fig. 1 Four-point location model for stereoselectivity of a protein, showing how a protein might provide two sites (D' and D'') in either of two locations for interaction with group D on a chiral carbon atom: D' would bind one enantiomer and D'' would bind its mirror image.11
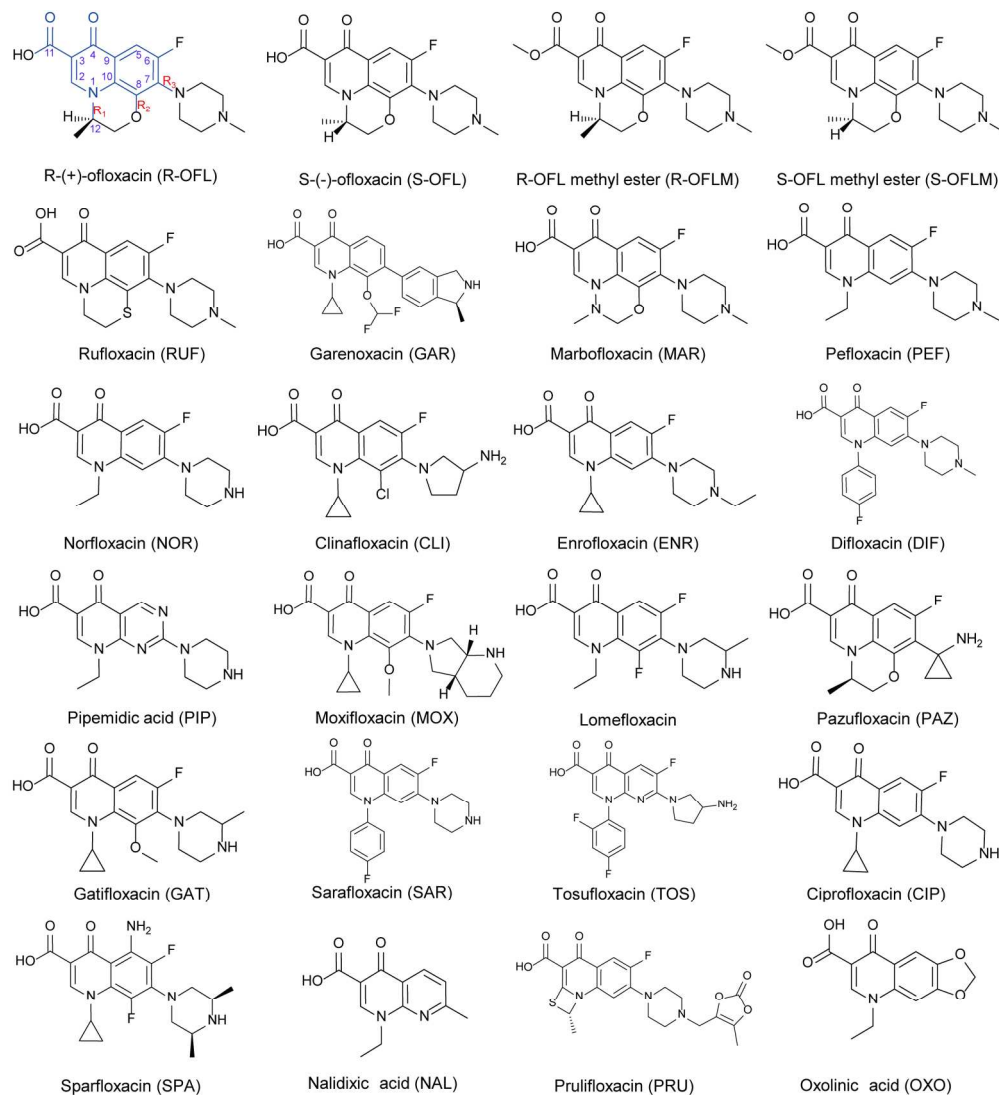50x32mm (300 x 300 DPI)

Fig. 2 The structure of QNs involved in this study. The common structure of QNs is labeled in blue.
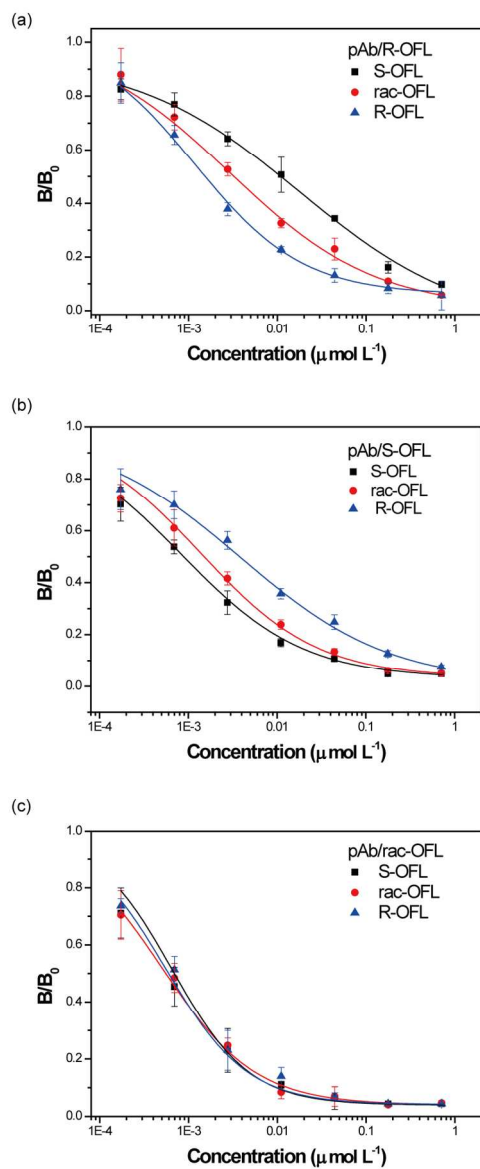171x186mm (300 x 300 DPI)

1
2
3
4
5
6
7
8
9
10
11
12
13
14
15
16
17
18
19
20
21
22
23
24
25
26
27
28
29
30
31
32
33
34
35
36
37
38
39
40
41
42
43
44
45
46
47
48
49
50
51
52
53
54
55
56
57
58
59
60

Fig. 3 Representative inhibition curves of pAb/R-OFL (a), pAb/S-OFL (b) and pAb/rac-OFL (c) by varying concentrations of free S-OFL(■), rac-OFL (●) and R-OFL(▲). Each point represents the mean ±SD (standard deviation) of three assays.
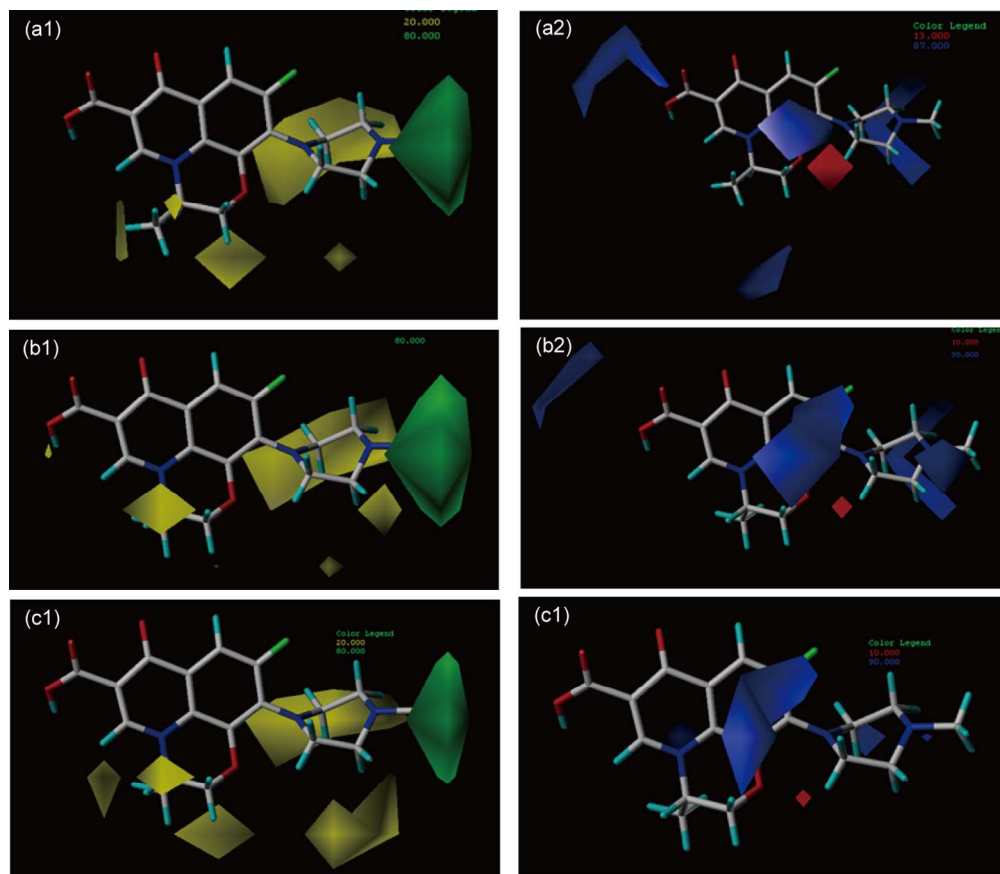83x174mm (300 x 300 DPI)

Fig. 4 CoMFA std*coeff contour plots of model pAb/R-OFL with R-OFL as reference molecule (a1, a2), pAb/S-OFL with S-OFL (b1, b2), and pAb/rac-OFL with S-OFL (c1, c2). In steric contour maps (a1, b1, and c1), green and yellow contours refer to sterically favored and unfavored regions; in electrostatic contour maps (a2, b2, and c2), blue and red contours refer to regions where electron-donating and electron withdrawing groups are favored.
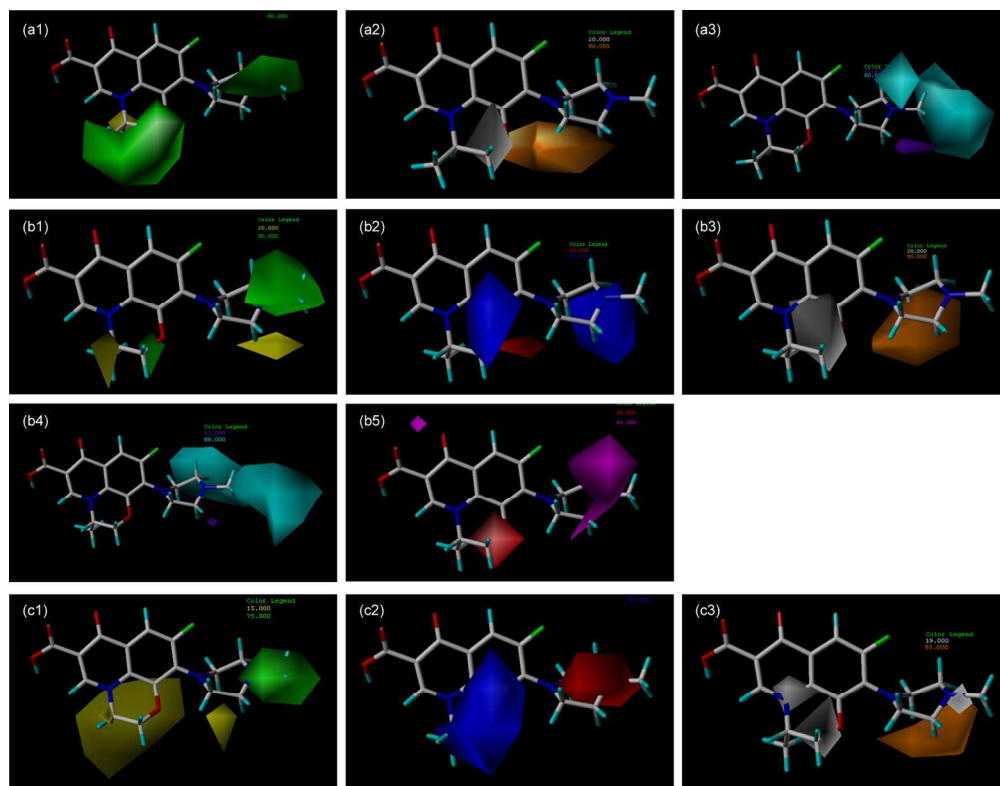120x104mm (300 x 300 DPI)

Fig. 5 CoMSIA std*coeff contour plots of model pAb/R-OFL with R-OFL as reference molecule (a1-a3), pAb/S-OFL with S-OFL (b1-b5), and pAb/rac-OFL with S-OFL (c1-c3). In steric contour maps (a1, b1, and c1), green and yellow contours refer to sterically favored and unfavored regions; in electrostatic contour maps (b2, c2), blue and red contours refer to regions where electron-donating and electron withdrawing groups are favored; in hydrophobic contour maps (a2, b3, and c3), white and orange contours refer to regions where hydrophilic and hydrophobic substituents are favored; in hydrogen bond donor contour maps (a3, b4), the cyan and purple contours indicate favorable and unfavorable hydrogen bond donor groups; in hydrogen bond acceptor contour map (b5), the magenta and red contours demonstrated favorable and unfavorable hydrogen bond acceptor groups.
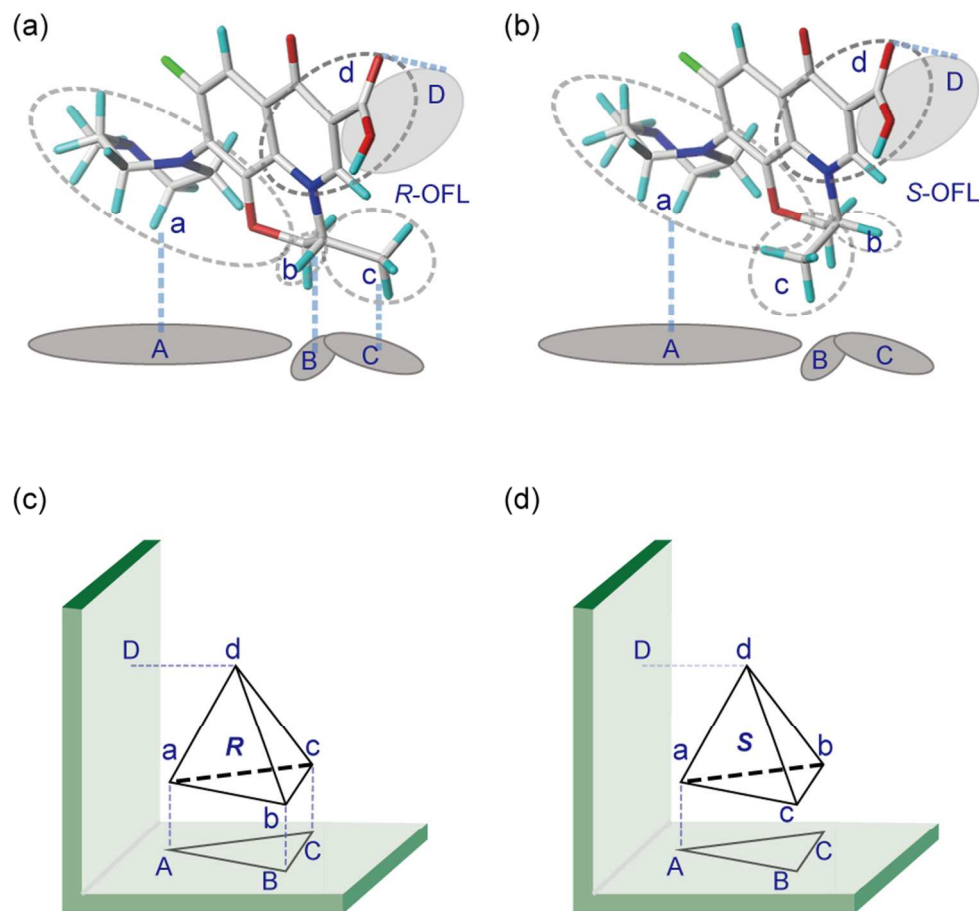171x133mm (300 x 300 DPI)

Fig. 6 Ofloxacin–antibody recognition model (a, b) and illustrative enhanced four-location model (c, d). The 4 groups attached to the tetrahedral C12 atom of ofloxacin are labeled by oval dashed lines; meanwhile, corresponding binding sites on antibody are represented by gray ovals. The dashed line in light blue represents interactions between enantiomer and antibody.

83x77mm (300 x 300 DPI)